Investigation of the Role of Reductant on the Size Control of Fe_3O_4 Nanoparticles on Rice Straw

Roshanak Khandanlou,[a] Mansor Bin Ahmad,[a,]* Kamyar Shameli,[a, b,]* and Katayoon Kalantari [a]

The goal of this study was to prepare nanocomposites of rice straw coated with different percentages of Fe_3O_4 nanoparticles (Fe_3O_4-NPs) [1.0, 5.0, 10.0, and 20.0 wt. %]. In this process, the size of Fe_3O_4-NPs changed with varying volumes of NaOH (2M). The Fe_3O_4-NPs were precipitated with sodium hydroxide from a solution of Fe(II) and (III) chloride in water under ambient conditions and N_2 gas by the quick precipitation method using urea as a stabilizer. The rice straw/Fe_3O_4 nanocomposites (NCs) prepared by this method had magnetic properties in percentages higher than ten (10 wt. %). When the volume of NaOH increased, Fe_3O_4-NPs with uniform size and better distribution could be prepared, which means that the size of the NPs decreased as the reducing agent was increased. Transmission electron microscopy (TEM) showed that Fe_3O_4-NPs in rice straw were spherical with diameters from 18.47 to 9.93 nm. The SEM results show that the structure of rice straw underwent no particular change. EDX indicated the presence of Fe_3O_4-NPs on the surface of rice straw. X-ray powder diffraction (PXRD) indicated that the magnetic Fe_3O_4-NPs were pure and that the particles were small. The FT-IR results showed that the Fe_3O_4-NPs were successfully coated on the surface of rice straw.

Keywords: Rice straw; Nanocomposites; Iron oxide; Nanoparticles; Transmission electron microscopy

Contact information: a: Department of Chemistry, Faculty of Science, Universiti Putra Malaysia, 43400 UPM Serdang, Selangor, Malaysia; b: Nanotechnology and Advance Department, Materials and Energy Research Center, Meshkin-Dasht Road, Karaj 3177983634, Iran;
** Corresponding authors: mansorahmad@gmail.com; kamyarshameli@gmail.com*

INTRODUCTION

With an availability of more than 580 million tons every year, rice straw is one of the most common sources of biomass existent in the world. Currently, there is very limited use of rice straw in the construction, agriculture, paper, packing, fuel, and energy industries. Most of the rice straw accessible after harvest is either left on the ground or burnt (Reddy and Yang 2006). Rice straw, mostly consisting of cellulose and hemicellulose, has been widely regarded as an important reproducible source for bioethanol, animal feedstock, and organic chemicals (Jin *et al.* 2007). It is one of the main cereal straws and is produced in large quantities world-wide every year. In developing countries, these large quantities of fibrous crop residues are currently under-utilized either as raw material for papermaking or as potential animal feed sources (Sun *et al.* 2000). Rice straw is not only a potential source of energy but also a value-added by-product (Fu *et al.* 2009). It represents around 45% of the volume in rice production, producing the largest quantity of crop residue. Rice straw has relatively high amount of cellulose from agricultural crop residues because of its composition: cellulose (38.3%), hemicelluloses (31.6%), and lignin (11.8%) (Hessien *et al.* 2009).

Nanoscience is one of the most important research and development frontiers in modern science. The use of nanoparticles (NPs) offers many advantages due to their unique size and physical properties. Because of the widespread applications of magnetic nanoparticles (MNPs) in biomedical, biotechnology, engineering, material science, and environmental areas, much attention has been paid to the preparation of different kinds of MNPs. NPs are submicron moieties (diameters ranging from 1 to 100 nm according to the used term, although there are examples of NPs several hundreds of nanometers in size) made of inorganic or organic materials, which have many novel properties compared with the bulk materials (Wu *et al.* 2008). Magnetic NPs have many unique magnetic properties, such as superparamagnetism, high coercivity, low Curie temperature, and high magnetic susceptibility. Magnetic NPs are of great interest for researchers from a broad range of disciplines, including magnetic fluids, data storage, catalysis, and bio-applications (Patel *et al.* 2008, Mornet *et al.* 2006, Stevens *et al.* 2005). MNPs have many applications in biomedical sciences and industries due to their convenient physical characteristics (Liu *et al.* 2004; Zahn 2001). Among different kinds of MNPs, investigations have focused on Fe_3O_4-NPs due to their enhanced chemical stability and biocompatibility compared to other metallic magnetic nanoparticles (Liu *et al.* 2009; MacCarthy and Weissleder 2008). Magnetite, Fe_3O_4, is an extensively studied material because of several interesting properties. It is ferromagnetic with a high Curie temperature of 858 K and electronically conducting with highly spin-polarized conduction electrons. Consequently, it is an interesting candidate for magnetic recording media or spin-valve applications (Tang *et al.* 2004).

Fe_3O_4-NPs are usually obtained by various chemical-based synthetic methods, including co-precipitation, the reverse micelle method, sol–gel techniques, freeze drying, ultrasound irradiation, hydrothermal methods, laser pyrolysis techniques, and thermal decomposition of organo-metallic and coordinated compounds (Yan *et al.* 2008).

Magnetite is a common magnetic iron oxide that has a cubic inverse spinel structure with fcc close packed oxygen anions and Fe cations occupying interstitial tetrahedral and octahedral sites (Karaoglu *et al.* 2011). Magnetite Fe_3O_4-NPs have received intense interest in recent years due to their potential application in various fields, such as ferro-fluids, catalysts, high-density magnetic recording media, and medical diagnostics (Chen *et al.* 2009). Because of their black color, surface chemistry, and strong magnetic properties, they have found a great number of applications in industry (Tartaj *et al.* 2003).

Studies on talc/Fe_3O_4-NCs (Kalantari *et al.* 2013a,b), rice straw/Fe_3O_4-NCs (Khandanlou *et al.* 2013), zeolite/Fe_3O_4-NCs (Jahangirian *et al.* 2013), and other nanoparticles such as silver in talc (Shameli *et al.* 2010a), montmorillonite (Shameli *et al.* 2010b, Ahmad *et al.* 2009a, Ahmad *et al.* 2009b), zeolite (Shameli *et al.* 2011a), montmorillonite/starch (Ahmad *et al.* 2010), chitosan (Ahmad *et al.* 2009c, 2011a,b; Shameli *et al.* 2011b), polyethylene glycol (Shameli *et al.* 2012a,b), plant extract (Shameli *et al.* 2012c,d), and polymeric substrate (Shameli *et al.* 2011c), have been previously reported.

In this work, rice straw/Fe_3O_4-NCs were prepared with different percentages of Fe_3O_4 (1.0, 5.0, 10.0, and 20.0 wt. %) at room temperature in aqueous solution using $FeCl_3 \cdot 6H_2O$ and $FeCl_2 \cdot 4H_2O$ and sodium hydroxide as iron precursors and a reduction agent, respectively. To date, there have been no reports of rice straw/Fe_3O_4-NCs synthesis using a chemical quick precipitation method, *i.e.*, using the exterior layer of rice straw fibers, which is the interest of this research.

EXPERIMENTAL

Materials

All chemical reagents used in this study were of analytical grade and used without further purification. Rice straw was obtained from a local farm (Bukit Tinggi, Kedah, Malaysia). Materials used for the synthesis of Fe_3O_4-NPs included the following: $FeCl_3 \cdot 6H_2O$ and $FeCl_2 \cdot 4H_2O$ (99.89%) were supplied by Merck (Frankfurter, Germany); urea (99%) was purchased from Hamburg Chemicals (Hamburg, Germany); NaOH (99.0%) was obtained from R & M Chemistry (Chicago, USA); and HNO_3 (70%) and HCl (37%) were obtained from Sigma-Aldrich (St Louis, MO, USA). All solutions were freshly prepared using double distilled water and kept in the dark to avoid any photo-chemical reactions. All glassware used in experimental procedures was cleaned in a fresh solution of HNO_3/HCl (3:1, v/v), washed thoroughly with double distilled water, and dried before use.

Synthesis of Rice Straw/Fe_3O_4Nanocomposites

For the synthesis of rice straw/Fe_3O_4-NCs, the samples consisted of 1.0, 5.0, 10.0, and 20.0 wt. % Fe_3O_4 in rice straw (2 g). Constant amounts of rice straw were suspended in deionized water, and then urea (2 M) was added to the mixtures. Different volumes of iron (II) and (III) chloride salts (Fe^{3+}:Fe^{2+}) with a molar ratio of 2:1 were added to this solution with vigorous stirring under nitrogen gas to prevent oxidation. Freshly prepared NaOH solutions (2 M) [1.0, 5.0, 10.0, and 20.0 mL] were then added to the suspensions with a molar ratio of 1:4 to prepare iron oxide. After addition of the reducing agent, stirring was continued for another hour. The Fe_3O_4-NPs were prepared in the basic pH, and were measured during the reaction process. The pH of rice straw after addition of urea was 5.71, because urea is a weak base. Then, the iron chloride and NaOH were added at different volumes and the pH ranged from 8 and 9. The suspensions were finally centrifuged, washed twice with ethanol and deionized water, and dried in an oven at 60 °C. All the experiments were conducted at ambient temperature. As shown in Fig. 1 (a–d), a magnet does not attract pure rice straw powder or rice straw/Fe_3O_4-NCs with 1.0,

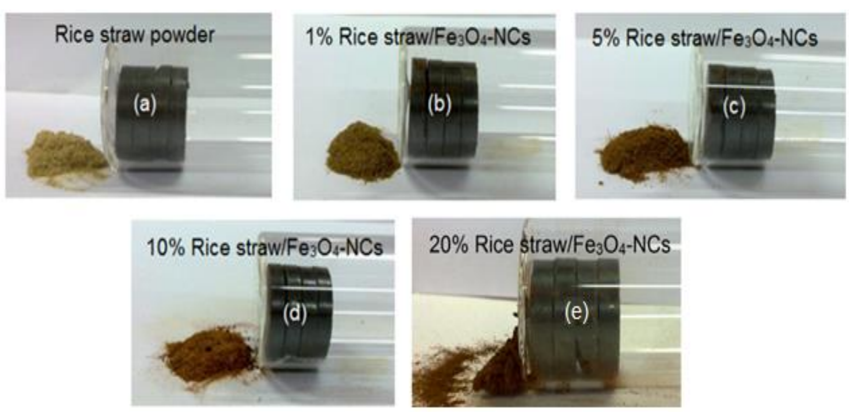

Fig. 1. Schematic illustration of the magnetic attraction of rice straw (a) and rice straw/Fe_3O_4-NCs at different NPs percentages [1.0, 5.0, 10.0, and 20.0 wt. % (b–e)]

5.0, and 10.0 wt. % Fe_3O_4, which indicates in the lowest percentage, the amount of NPs that are coated on the surface of rice straw is lower than rice straw; therefore rice straw does not allow the NPs to be attracted to the magnet, even if this composite has magnetic properties. Fe_3O_4-NPs at 20.0 wt. %, which were formed on the surface of the rice straw, are attracted by the magnet [Fig. 1(e)].

Characterization Methods and Instruments

Transmission electron microscopy (TEM) was used to measure the morphology and size of samples obtained. A drop of diluted sample in distilled water was dripped onto a covered copper grid. TEM observations were carried out using a Hitachi H-7100 electron microscope, and the particle size distributions were determined using the UTHSCSA Image Tool software, version 3.00. Electron field-emission scanning electron microscopy (FESEM) was applied to observe the morphology of rice straw and rice straw/Fe_3O_4-NCs. FESEM with energy-dispersive X-ray fluorescence (EDXF) spectroscopy was performed with a JEOL JSM-7600F instrument. Powder X-ray diffraction (PXRD) with Cu Kα radiation was used to measure the crystallinity of samples. Fourier transform infrared spectroscopy (FT-IR) in the range of 400 to 4000 cm^{-1} was used to study the structures of the rice straw, urea, and rice straw/Fe_3O_4-NCs. FT-IR spectra were recorded utilizing a Series 100 PerkinElmer FT-IR 1650 spectrophotometer.

RESULTS AND DISCUSSION

The effectiveness of the reducing agent in the synthesis of NPs could be evaluated by the size and size distribution of the prepared NPs. Figure 2 gives an overview of the synthesis of rice straw/Fe_3O_4-NCs. The color of the prepared NCs gradually changed from light brown for rice straw to black for rice straw/Fe_3O_4-NCs, which indicated the formation of Fe_3O_4-NPs on the surface of the rice straw. The observation of a slow color change from light brown to dark brown, and then the abrupt transition from brown to black afterwards, suggested that the reaction could indeed follow zero-order kinetics once the nuclei had formed in the solution (Teng and Yang 2004).

The chemical reactions of Fe_3O_4 in the surface of rice straw are given in below equations (1, 2). The overall reaction may be written as follows.

$$\text{Rice straw} + H_2O_{(L)} + 2Fe^{3+}_{(aq)} + Fe^{2+}_{(aq)} \xrightarrow{Stirring} [\text{Rice straw} /2Fe^{3+}: 1Fe^{2+}] \quad (1)$$

$$[\text{Rice straw} /2Fe^{3+}: 1Fe^{2+}] + 8OH^{-}_{(aq)} \rightarrow [\text{Rice straw} /Fe_3O_4]\downarrow_{(s)} + 4H_2O_{(L)} \quad (2)$$

Comparison of the PXRD patterns of rice straw and rice straw/Fe_3O_4-NCs (Fig. 3) showed the formation of Fe_3O_4-NPs on the surface of the rice straw. The TEM images and size distributions of rice straw/Fe_3O_4-NCs showed that the mean diameter of the NPs ranged from 18.47 to 9.93 nm (Fig. 4). The FESEM images of rice straw/Fe_3O_4-NCs show good dispersion of NPs on the surface of the rice straw (Fig. 5). FT-IR analysis of prepared NCs revealed the presence of Fe on the surface of the rice straw (Fig. 6).

Powder X-Ray Diffraction Analysis

A comparison of the PXRD patterns of the rice straw and rice straw/Fe_3O_4-NCs prepared by the quick precipitation method in the small angle range of 2θ=15–25° indicated the formation of an intercalated Fe_3O_4 nanostructure [Fig. 3 (a–e)]. When the percentage of Fe_3O_4-NPs formed on the surface of the rice straw was increased, the intensity of these peaks was decreased. The broad diffraction peak centered at 22.20° is attributed to rice straw; all the rice straw/Fe_3O_4-NCs had a similar diffraction profile, and the PXRD peaks at 2θ 30.45°, 35.86°, 43.48, 53.82°, 57.02°, 63.22°, 73.78°, and 89.52° could be attributed to the 220, 311, 400, 422, 511, 440, 533, and 731 crystallographic planes of face-centered cubic (fcc) iron crystals, respectively (Daraei *et al.* 2012). These peaks are consistent with the reference code Fe_3O_4 01-088-0315 and reveal that the reaction product was pure Fe_3O_4-NPs.

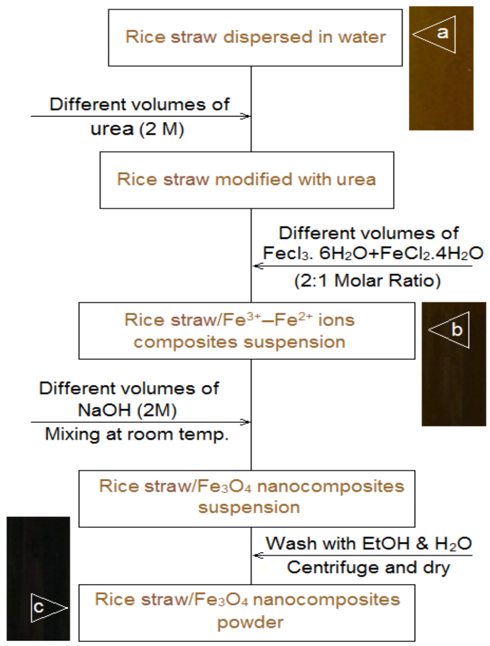

Fig. 2. Flowchart of the rice straw (a) and synthesized rice straw/Fe_3O_4-NCs (b–c)

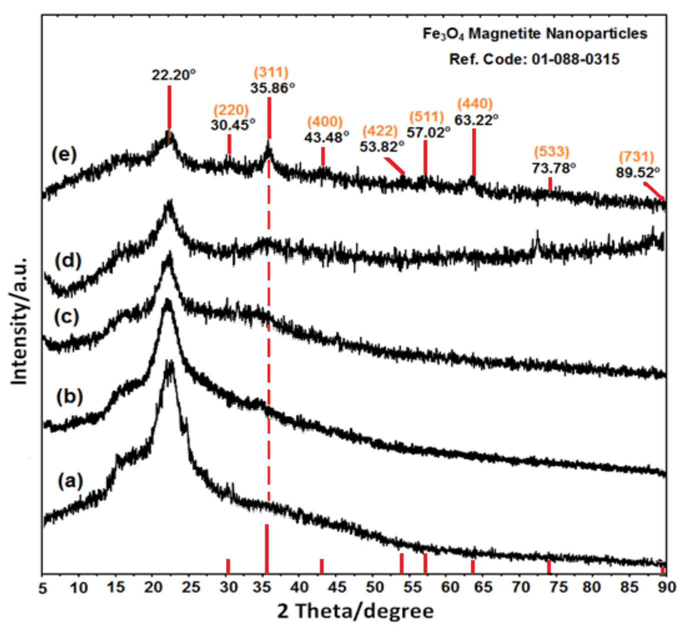

Fig. 3. PXRD of rice straw (a) and rice straw/Fe_3O_4-NCs [1.0, 5.0, 10.0, and 20.0 wt. % (b–e)]

With increasing amounts of Fe_3O_4-NPs, the height of peaks in the range of 2θ = 30 to 90° increased. To investigate the effect of reducing agent on the size of NPs, different amounts of NaOH and iron salts were utilized, with a fixed time and reaction temperature. The increasing volume concentration of NaOH led to regular increases in peak intensities and a gradual decrease in particle size. One possible reason for this is that the repulsive force between hydroxide ions hinders the growth of crystal grains when the excess hydroxide ions produced from NaOH are adsorbed on the surface of the crystal nuclei (Yan *et al.* 2009).

The particle sizes can be quantitatively evaluated from the XRD data using the *Debye-Scherrer* equation,

$$n = K\lambda / \beta \cos\theta \quad (3)$$

where K is Scherrer's constant with a value from 0.9 to 1 (shape factor), λ is the X-ray wavelength (1.5418 Å), $\beta_{1/2}$ is the width of the XRD peak at half height, and θ is the Bragg angle. From Scherrer's equation, the average crystallite size of Fe_3O_4-NPs for rice straw/Fe_3O_4-NCs with 1.0, 5.0, 10.0, and 20.0 wt. % are around 10 to 20 nm, in agreement with TEM and FESEM results discussed later.

Morphological Studies

TEM micrographs of rice straw/Fe_3O_4-NCs containing different loading percentages and a calculated histogram are shown in Fig. 4. The TEM images and their size distributions showed that the mean diameters and standard deviations of Fe_3O_4-NPs were about 18.47±3.68, 14.18±2.96, 11.79±3.44, and 9.93±2.42 nm for 1.0, 5.0, 10.0, and 20.0 wt.% [Fig. 4 (a–d)], respectively. These results show when the amount of reducing agent and, therefore, percentage loading were increased, the average particle size of Fe_3O_4-NPs gradually decreased and the dispersal of Fe_3O_4-NPs was much better in the rice straw matrix, although particles seem to aggregate to some extent in higher concentrations. It can be seen that the Fe_3O_4-NPs exhibit spherical morphology, which agrees well with the results of XRD. Importantly, no morphological differences were observed between the rice straw and rice straw/Fe_3O_4-NCs. Usually, spherical shapes are formed. This is because the nucleation rate per unit area is isotopic at the interface between the Fe_3O_4 magnetic nanoparticles, which is the driving force for Ostwald ripening; minimization of the surface free energy by reduction of total surface area to volume ratio results in an equivalent growth rate along different directions of nucleation because the sphere has the smallest surface area per unit volume of any shape (Lu *et al.* 2010). The numbers of Fe_3O_4-NPs counted for TEM images were around 131, 273, 346 and 385, respectively.

Figure 5 shows the surface morphology of rice straw and rice straw/Fe_3O_4-NCs (a–e). In the rice straw image (Fig. 5a), no morphological differences were observable between the initial rice straw and the rice straw/Fe_3O_4-NCs. As shown in the images, uniformly prepared rice straw/Fe_3O_4-NCs consisted of spherical particles, which was consistent with the TEM results. With increasing Fe_3O_4-NPs loading percentage, particles appeared to aggregate together, but they exhibited good dispersion. The NPs were uniform, and the average particle size was smaller at lower loading percentages. These results confirm that the modified surface of rice straw can effectively control the shape and size of the Fe_3O_4-NPs. The surfaces of rice straw/Fe_3O_4-NCs with high magnification gradually become shiny. This was due to the presence of small size Fe_3O_4-NPs, which could aggregate together and create large particles of Fe_3O_4-NPs.

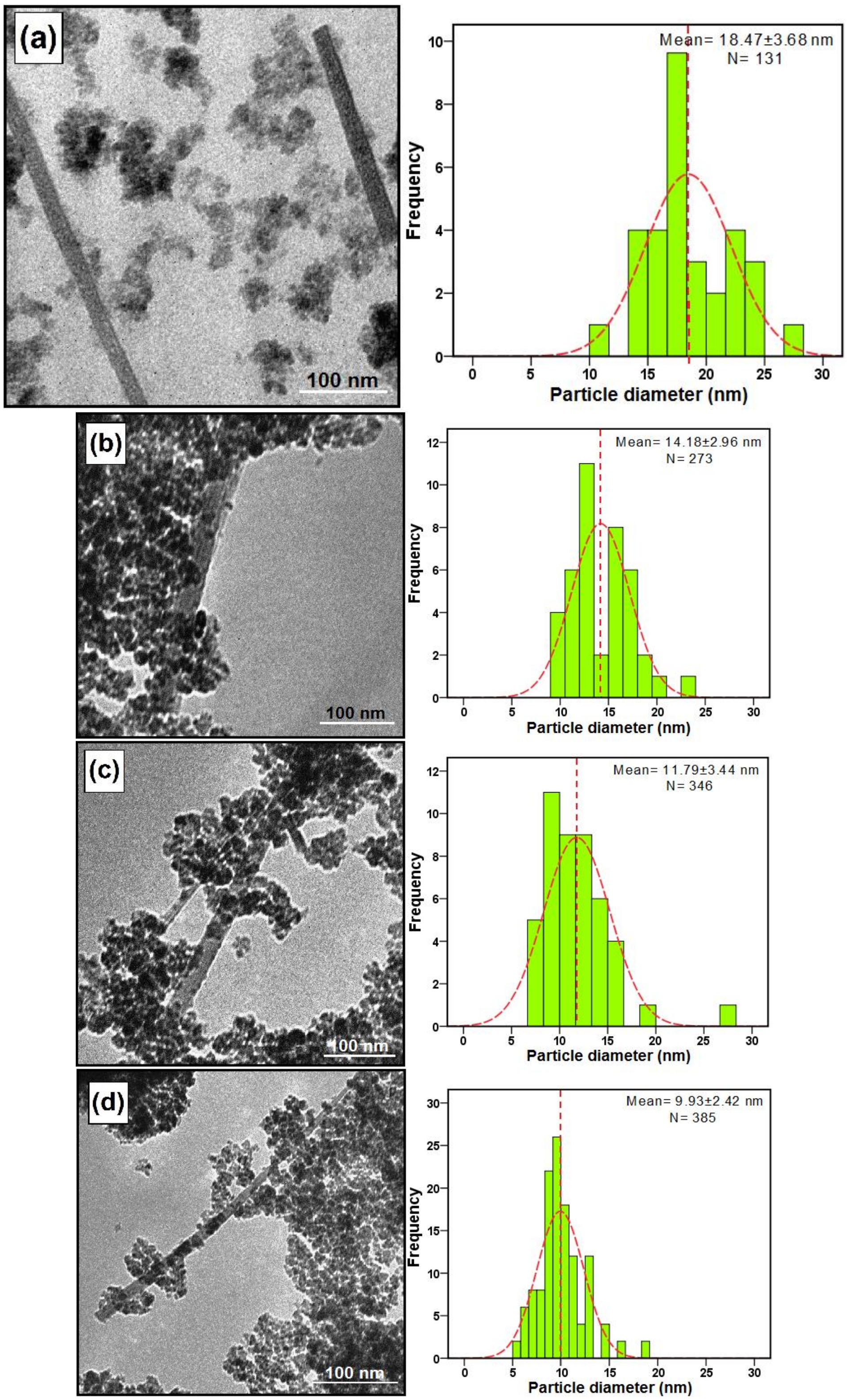

Fig. 4. Transmission electron microscopy images and corresponding particle size distribution of rice straw/Fe_3O_4-NCs at different Fe_3O_4 percentages [1.0, 5.0, 10.0, and 20.0 wt. % (a–d)]

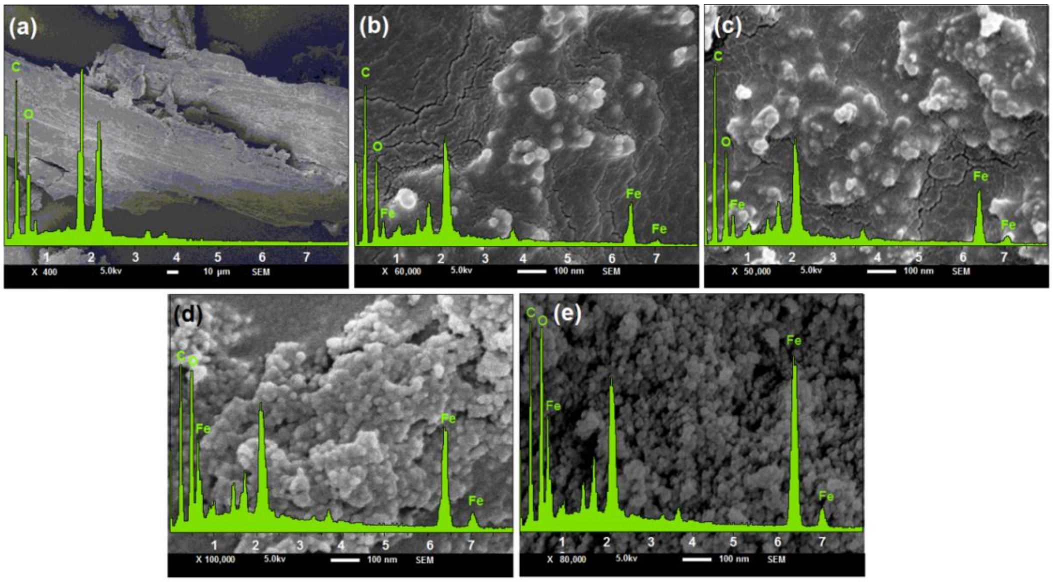

Fig. 5. Scanning electron microscopy images and energy dispersive X-ray spectroscopy of rice straw (a) and rice straw/Fe_3O_4-NCs peaks in 1.0, 5.0, 10.0, and 20.0 wt. % of Fe_3O_4 (b–e)

The chemical compositions of the as-prepared rice straw and rice straw/Fe_3O_4-NCs were analyzed by EDX. Figure 5a shows a carbon peak (C) at 0.24 keV and an oxygen peak (O) at 0.4 keV in rice straw. After the coating of Fe_3O_4-NPs on the rice straw surface, the Fe peaks appeared in the EDX. The iron peaks (Fe) appear at 0.68, 6.20, and 7.30 keV in all samples of rice straw/Fe_3O_4-NCs [Fig. 5(b–e)] (Bhaumik *et al.* 2011). The peaks at 1.75 to 2.25 keV are related to gold which were used for sample coating. With increasing Fe_3O_4-NPs percentage, the height of the iron peak and the amount of NPs that were coated on the rice straw surface increased. Therefore, EDX analyses provide direct evidence for adsorption of iron oxide on the surface of rice straw.

FT-IR Chemical Analysis

Figure 6 shows the FT-IR spectra of rice straw and rice straw/Fe_3O_4-NCs with different concentrations of Fe_3O_4-NPs. In the IR spectrum of raw rice straw (Fig. 6a), the absorption peaks at 3377 cm^{-1} and 2933 cm^{-1} are ascribed to stretching vibrations of –OH groups and C–H stretching, respectively (Chen *et al.* 2011). The smaller shoulder peak at 1735 cm^{-1} in the rice straw is attributed to aliphatic esters in lignin or hemicelluloses. The intense band at 1646 cm^{-1} is assigned to olefinic C=C stretching vibrations (Qin *et al.* 2011). The peak at 1444 cm^{-1} is ascribed to the aromatic C=C stretch of aromatic vibrations in bound lignin. The absorbance peaks in the 1376 to 1363 cm^{-1} region originate from C–H bending. The region of 1200 to 1000 cm^{-1} represents C–O stretching and deformation bands in cellulose, lignin, and residual hemicelluloses (Sun *et al.* 2005).

In the FT-IR spectrum of urea (Fig. 6f), absorption peaks at 3429 cm^{-1} and 3329 cm^{-1} are ascribed to stretching of –NH_2 groups. The intense band at 1591 cm^{-1} is assigned to bending vibration of the N–H group, which overlaps with the vibration band of the carbonyl group. The band at 1452 cm^{-1} is assigned to the stretching of the C–N group. The presence of Fe_3O_4-NPs on the surface of rice straw is evidenced by the adsorption bands at around 301 to 541 cm^{-1} in 1.0, 5.0, 10.0, and 20.0 wt. % Fe_3O_4-NPs, confirmed by the Fe–O stretching (Bahçeci *et al.* 2011). Absorption peaks at 3334, 3329, 3337, 3340, and 3334 cm^{-1}, the associated hydroxyl groups, indicate the existence of rice straw.

With increasing Fe_3O_4-NPs loading percentage, the intensity of adsorption peaks in all rice straw/Fe_3O_4-NCs samples decreased. One possible reason for this decrease in intensity is that when Fe_3O_4-NPs are coated on the rice straw surface, the pure rice straw is partially reduced (Chang *et al.* 2012). The FT-IR spectra indicated the non-bond chemical interaction between rice straw, urea, and Fe_3O_4-NPs. The interaction between rice straw, urea, and Fe_3O_4-NPs is indicated *via* the decrease in intensity of –OH groups in rice straw. The decrease in intensity of peaks can be attributed to substantial structural disorder at the surface of the nanoparticles. The degree of disorder and distortion is expected to increase with decreasing particle size (Shido and Prins 1998). The magnitude of the FT-IR peak is inversely related to the Debye-Waller factor corresponding to the mean square relative displacement of the inter-atomic distance due to static disorder and thermal vibrational disorder (Zhang *et al.* 2011; Choi *et al.* 2002). For all samples, the peaks shifted to lower wave numbers with increased Fe_3O_4-NPs percentage. This result indicates that Fe_3O_4-NPs can be successfully coated on the surface of rice straw.

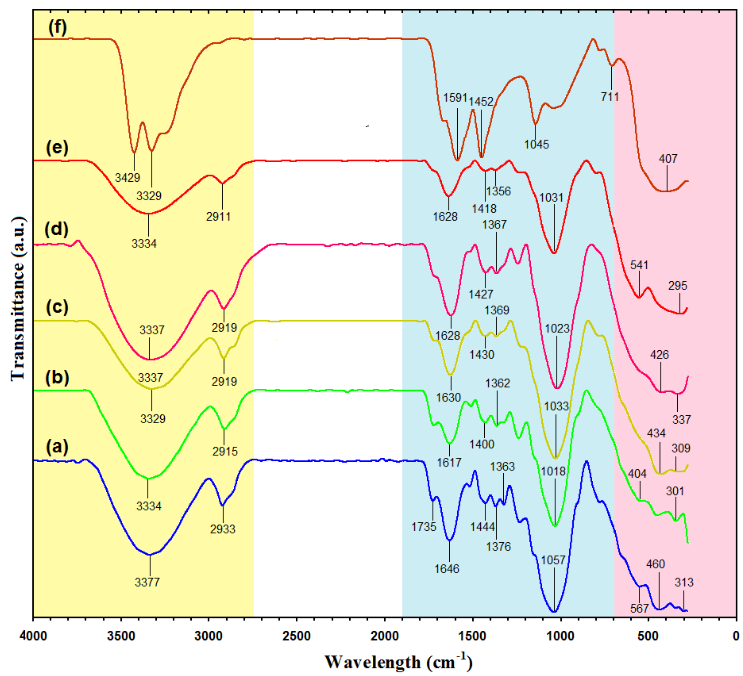

Fig. 6. Fourier transform infrared spectra of rice straw (a), rice straw/Fe_3O_4–NCs, and urea peaks with 1.0, 5.0, 10.0, and 20.0 wt. % Fe_3O_4 (b–f)

In the finger print region, rice straw exhibited peaks and also rice straw/Fe_3O_4-NCs with 1, 5, and 10 wt.% (b-d) in this region showed peaks that overlapped with the peaks of rice straw. The peaks could not be clearly differentiated because the percentages of Fe_3O_4-NPs were not very high, and the peaks could overlap with those of rice straw. Also, while Fe-O shows a peak at 1624 cm^{-1} (Lu *et al*. 2010), again in this region rice straw has a peak, so due to the overlapping of Fe-O peaks with the peaks of rice straw, the Fe-O stretching cannot be seen in the FT-IR spectrum from 5 to 10 wt.% Fe_3O_4-NPs. In the case of 20 wt.% (e) of NPs the peak at 541 cm^{-1} indicated Fe-O stretching (Shen *et al*. 2012), because the amount of NPs was sufficiently high. The Fe-O stretching could show itself as a peak emerging from the overlapping peaks of rice straw.

On the basis of the above results, with respect to the formation of Fe_3O_4-NPs, it can be seen in Fig. 7 that urea was adsorbed on the surface of rice straw *via* hydrogen bonding between the –OH groups of rice straw and the carbonyl group of urea. Also, urea has two NH_2 groups, which have negative dipole moments, and the surface of Fe_3O_4-NPs has a partial positive charge, so these two negative and positive charges can attract each other.

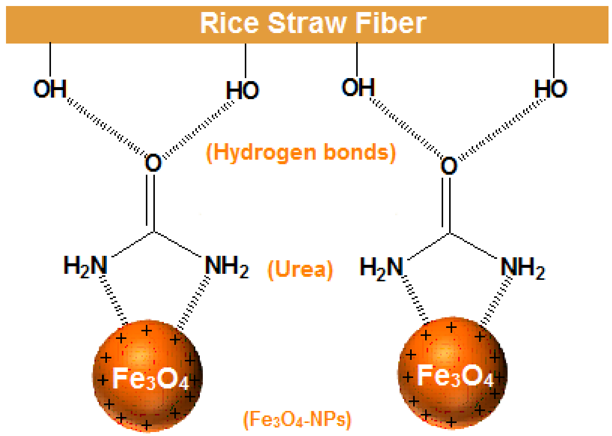

Fig. 7. Schematic illustrations of the synthesis of Fe_3O_4-NPs on the surface of modified rice straw

CONCLUSIONS

1. Four samples of rice straw/Fe_3O_4-NCs were prepared by co-precipitation of ferrous and ferric ions using sodium hydroxide as a precipitating agent. The reactant and product could be treated in an oxygen-free atmosphere to avoid unfavorable oxidation of the reactant and product by oxygen. N_2 gas was used to remove oxygen from the media.
2. The amount of NaOH had a significant effect on the size, dispersion, and magnetic properties of the Fe_3O_4-NPs. By increasing of NaOH volume concentration, Fe_3O_4-NPs with regular size and good distribution could be prepared.
3. When the amounts of reducing agent were increased, the crystal structures of NPs were decreased. The spherical shape and sizes of metal oxide NPs with diameters from 18.47 to 9.93 nm, were determined by TEM.

ACKNOWLEDGEMENTS

The authors thank University Putra Malaysia (UPM) for its financial support (RUGS, Project No. 9199840). The authors are also grateful to the staff of the Department of Chemistry UPM for their help in this research, and to the Institute of Bioscience (IBS/UPM) for technical assistance.

REFERENCES CITED

Ahmad, M. B., Shameli, K., Wan Yunus, W. M. Z., Ibrahim, N. A., Hamid, A. A., and Zargar, M. (2009a). "Synthesis and antibacterial activity of silver/montmorillonite nanocomposites," *Res. J. Biol. Sci.* 4(9), 1032-1036.

Ahmad, M. B., Shameli, K., Wan Yunus, W. M. Z., and Ibrahim, N. A. (2009b). "Synthesis and characterization of silver/clay nanocomposites by chemical reduction method," *Am. J. Appl. Sci.* 6(11), 1909-1914.

Ahmad, M. B., Shameli, K., Wan Yunus, W. M. W., Ibrahim, N. A., Hamid, A. A., and Zargar, M. (2009c). "Antibacterial activity of silver/clay/chitosan bionanocomposites," *Res. J. Biol. Sci.* 4(11), 1156-1161.

Ahmad, M. B., Shameli, K., Wan Yunus, W. M. Z., and Ibrahim, N. A. (2010). "Synthesis and characterization of silver/clay/starch bionanocomposites by green method," *Aust. J. BasicAppl.Sci.* 4(7), 2158-2165.

Ahmad, M. B., Lim, J. J., Shameli, K., Ibrahim, N. A., and Tay, M. Y. (2011a). "Synthesis of silver nanoparticles in chitosan, gelatin and chitosan/gelatin bionanocomposites by a chemical reducing agent and their characterization," *Molecules* 16(9), 7237-7248.

Ahmad, M. B., Tay, M. Y., Shameli, K., Hussein, M. Z., and Lim, J. J. (2011b). "Green synthesis and characterization of silver/chitosan/polyethylene glycol nanocomposites without any reducing agent," *Int. J. Mol. Sci.* 12(8), 4872-4884.

Bahçeci, S., Unal, B., Baykal, A., Sözeri, H., Karaoglu, E., and Esat, B. (2011). "Synthesis and characterization of polypropiolate sodium (PPNa)–Fe_3O_4 nanocomposite," *J. Alloys Compd.* 509(35), 8825-8831.

Bhaumik, M., Maity, A., Srinivasu, V. V., and Onyango, M. S. (2011). "Enhanced removal of Cr (VI) from aqueous solution using polypyrrole/Fe_3O_4 magnetic nanocomposites," *J. Hazard Mater.* 190(1-3), 381-390.

Chang, Y. P., Ren, C. L., Qu, J. C., and Chen, X. G. (2012). "Preparation and characterization of Fe_3O_4/graphene nanocomposite and investigation of its adsorption performance for aniline and p-chloroaniline," *Appl. Surf. Sci.* 261, 504-509.

Chen, J., Wang, F., Huang, K., Liu, Y., and Liu, S. (2009). "Preparation of Fe_3O_4 nanoparticles with adjustable morphology," *J. Alloys Compd.* 475(1-2), 898-902.

Chen, X., Yu, J., Zhang, Z. H., and Lu, C. (2011). "Study on structure and thermal stability properties of cellulose fibers from rice straw," *J. Carbohyd. Polym.* 85(1), 245-250.

Choi, H. C., Lee, S. Y., Kim, S. B., Kim, M. G., Lee, M. K., Shin, H. J., and Lee, J. S. (2002). "Local structural characterization for electrochemical insertion extraction of lithium in to CoO with X-ray absorption spectroscopy," *J. Phys. Chem.* 106(36), 9252-9260.

Daraei, P., Madaeni, S., Ghaemi, N., Salehi, E., Khadivi, M. A., Moradian, R., and Astinchap, B. (2012). "Novel polyethersulfone nanocomposite membrane prepared by PANI/Fe_3O_4 nanoparticles with enhanced performance for Cu (II) removal from water," *J. Membrane. Sci.* 415-416(19), 250-259.

Fu, P., Hu, S., Xiang, J., Sun, L. S., Yang, T., Zhang, A. C., and Zhang, J. Y. (2009). "Mechanism study of rice straw pyrolysis by Fourier transform infrared technique," *Chin. J. Chem. Eng.* 17(3), 522-529.

Hessien, M. M., Rashad, M. M., Zaky, R. R., Abdel-Aal, E. A., and El-Barawy, K. A. (2009). "Controlling the synthesis conditions for silica nanosphere from semi-burned rice straw," *J. Mater. Sci. Eng. B-ADV.* 162(1), 14-21.

Jahangirian, H., Shah Ismail, M. H., Haron, M. J., Rafiee-Moghaddam, R., Shameli, K., Hosseini, S., Kalantari, K., Khandanlou, R., Gharibshahi, E., and Soltaninejad, S. (2013). "Synthesis and characterization of zeolite/Fe_3O_4nanocomposites by green quick precipitation method," *Dig. J. Nanomaterials Bios.* 4. 8(4), 1405-1413.

Jin, S., and Chen, H. (2007). "Near-infrared analysis of the chemical composition of rice straw," *Ind. Crops Prod.* 26(2), 207-211.

Kalantari, K., Ahmad, M. B., Shameli, K., and Khandanlou, R. (2013a). "Synthesis of talc/Fe_3O_4 magnetic nanocomposites using chemical co-precipitation method," *Int. J. Nanomed.* 8, 1817-1823.

Kalantari, K., Ahmad, M. B., Shameli, K., and Khandanlou, R. (2013b). "Size-controlled synthesis of Fe_3O_4 magnetite nanoparticles on the exterior of talc layers," *Res. Chem. Intermediat.*1-13. (DOI 10.1007/s11164-013-1336-4)

Karaoglu, E., Baykal, A., Erdemi, H., Alpsoy, L., and Sozeri, H. (2011). "Synthesis and characterization of DL-thioctic acid (DLTA)–Fe_3O_4 nanocomposite," *J. Alloys Compd.* 509(37), 9218-9225.

Khandanlou, R., Ahmad, M. B., Shameli, K., and Kalantari, K. (2013). "Synthesis and characterization of rice straw/Fe_3O_4 nanocomposites by a quick precipitation method," *Molecules* 18(6), 6597-6607.

Liu, Z. L., Wang, H. B., Lu, Q. H., Du, G. H., Peng, L., Du, Y. Q., Zhang, S. M., and Yao, K. L. (2004). "Synthesis and characterization of ultrafine well-dispersed magnetic nanoparticles," *J. Magn. Magn. Mater.* 283(2-3), 258-262.

Liu, Z., Ding, J., and Xue, J. (2009). "A new family of biocompatible and stable magnetic nanoparticles: Silica cross-linked pluronic F127 micelles loaded with iron oxides," *New J. Chem.* 33(1), 88-92.

Lu, W., Shen, Y., Xie, A., and Zhang, W. (2010). "Green synthesis and characterization of super paramagnetic Fe_3O_4 nanoparticles," *J. Magn. Magn. Mater.* 322(13), 1828-1833.

MacCarthy, J. R., and Weissleder, R. (2008). "Multifunctional magnetic nanoparticles for targeted imaging and therapy," *Adv. Drug Deliv. Rev.* 60(11), 1241-1251.

Mornet, S., Vasseur, S., Grasset, F., Veverka, P., Goglio, G., Demourgues, A., Portier, J., Pollert, E., and Duguet, E. (2006). "Magnetic nanoparticle design for medical applications," *Prog. Solid State Chem.* 34(2-4), 237-247.

Patel, D., Moon, J., Chang, Y., Kim, T., and Lee, G. (2008). "Poly (d,l-lactide-co-glycolide) coated super paramagnetic iron oxide nanoparticles: Synthesis, characterization and in vivo study as MRI contrast agent," *Colloid Surf. A.* 313-314(1), 91-94.

Qin, L., Qiu, J., Liu, M., Ding, S., Shao, L., Lü, S., Zhang, G., Zhao, Y., and Fu, X. (2011). "Mechanical and thermal properties of poly(lactic acid) composites with rice straw fiber modified by poly(butyl acrylate)," *Chem. Eng. J.* 166(2), 772-778.

Reddy, N., and Yang, Y. (2006). "Properties of high-quality long natural cellulose fibers from rice straw," *J. Agric. Food Chem.* 54(21), 8077-8081.

Shen, M., Cai, H., Wang, X., Cao, X., Li, K., Wang, S. H., Guo, R., Zheng, L., Zhang, G., and Shi, X. (2012). "Facile one-pot preparation, surface functionalization, and toxicity assay of APTS-coated iron oxide nanoparticles," *Nanothecnol.* (10), 1-10.

Shameli, K., Ahmad, M. B., Wan Yunus, W. M. Z., and Ibrahim, N. A. (2010a). "Synthesis and characterization of silver/talc nanocomposites using the wet chemical reduction method," *Int. J. Nanomed.* 5, 743-751.
Shameli, K., Ahmad, M. B., Wan Yunus, W. M. Z., Ibrahim, N. A., Gharayebi, Y., and Sedaghat, S. (2010b). "Synthesis of silver/montmorillonite nanocomposites using γ-irradiation," *Int. J. Nanomed.* 5, 1067-1077.
Shameli, K., Ahmad, M. B., Zargar, M., Wan Yunus, W. M. Z., and Ibrahim, N. A. (2011a). "Fabrication of silver nanoparticles doped in the zeolite framework and antibacterial activity," *Int. J. Nanomed.* 6, 331-341.
Shameli, K., Ahmad, M. B., Zargar, M., Wan Yunus, W. M. Z., Ibrahim, N. A. Shabanzadeh, P., and Ghaffari Moghaddam, M. (2011b). "Synthesis and characterization of silver/montmorillonite/chitosan bionanocomposites by chemical reduction method and their antibacterial activity," *Int. J. Nanomed.* 6, 271-284.
Shameli, K., Ahmad, M. B., Wan Yunus, W. M. W., Ibrahim, N. A., and Jokar, M. (2011c). "Synthesis and characterization of silver/polylactide nanocomposites," *Proc. World Acad. Sci. Eng. Technol.* 64, 28-32.
Shameli, K., Ahmad, M. B., Jazayeri, S. D., Shabanzadeh, P., Jahangirian, H., Mahdavi, M., and Abdullahi, Y. (2012a). "Synthesis and characterization of polyethylene glycol mediated silver nanoparticles by the green method," *Int. J. Mol. Sci.* 13(6), 6639-6650.
Shameli, K., Ahmad, M. B., Jazayeri, S. D., Shabanzadeh, P., Sangpour, P., Jahangirian, H., and Gharayebi, Y. (2012b). "Investigation of antibacterial properties silver nanoparticles prepared via green method," *Chem. Cent. J.* 6(1) 1-10.
Shameli, K., Ahmad, M. B., Jaffar Al-Mulla, E. A., Ibrahim, N. A., Shabanzadeh, P., Rustaiyan, A., Abdollahi, Y., Bagheri, S., Sanaz, A., SaniUsman, M., and Zidan, M. (2012c). "Green biosynthesis of silver nanoparticles using *Callicarpa maingayi* stem bark extraction," *Molecules* 17(7), 8506-8517.
Shameli, K., Ahmad, M. B., Zamanian, A., Sangpour, P., Shabanzadeh, P., Abdollahi, Y., and Zargar, M. (2012d). "Green biosynthesis of silver nanoparticles using *Curcuma longa* tuber powder," *Int. J. Nanomed.* 7, 5603-5610.
Shido, T., and Prins, R. (1998). "Why EXAFS underestimated the size of small supported MoS_2 particles," *J. Phys. Chem.* 102(43), 8426-8435.
Stevens, P. D., Fan, J., Gardimalla, H. M. R., Yen, M., and Gao, Y. (2005). "Super paramagnetic nanoparticle-supported catalysis of suzuki cross-coupling reactions," *Lett.* 7(11), 2085-2088.
Sun, R. C., Tomkinson, J., Ma, P. L., and Liang, S. F. (2000). "Comparative study of hemicelluloses from rice straw by alkali and hydrogen peroxide treatments," *Carbohyd. Polym.* 42(2), 111-122.
Sun, X. F., Xu, F., Sun, R. C., Fowler, P., and Baird, M. S. (2005). "Characteristics of degraded cellulose obtained from steam-exploded wheat straw," *Carbohyd. Res.* 340(1), 97-106.
Tang, N. J., Zhong, W., Jiang, H. Y., Wu, X. L., Liu, W., and Du, Y. W. (2004). "Nanostructured magnetite (Fe_3O_4) thin films prepared by sol–gel method," *J. Magn. Magn. Mater.* 282(SI), 92-95.
Tartaj, P., Morales, M. P., Vientemillas-Verdaguer, S., Gonzalez-Carreno, T., and Serna, C. J. (2003). "The preparation of magnetic nanoparticles for applications in biomedicine," *J. Phys. D. Appl. Phys.* 36(13), 182-197.

Teng, X., and Yang, H. (2004). "Effects of surfactants and synthetic conditions on the sizes and self-assembly of monodisperse iron oxide nanoparticles," *J. Mater. Chem.* 14(4), 774-779.
Wu, W., He, Q., and Jiang, C. (2008). "Magnetic iron oxide nanoparticles: Synthesis and surface functionalization strategies," *Nanoscale Res. Lett.* 3(11), 397-415.
Yan, A., Liu, X., Qiu, G., Wu, H., Yi, R., Zhang, N., and Xua, J. (2008). "Solvo-thermal synthesis and characterization of size-controlled Fe_3O_4 nanoparticles," *J. Alloys Compd.* 458(1-2), 487-491.
Yan, H., Zhang, J., You, C., Song, Z., Yu, B., and Shen, Y. (2009). "Influences of different synthesis conditions on properties of Fe_3O_4 nanoparticles," *Mater. Chem. Phys.* 113(1), 46-52.
Zahn, M. (2001). "Magnetic fluid and nanoparticle applications to nanotechnology," *J. Nanopart. Res.* 3(1), 73-78.
Zhang, M., Pan, G., Zhao, D., and He, G. (2011). "XAFS study of starch-stabilized magnetite nanoparticles and surface speciation of arsenate," *Environ. Pollut.* 159(12), 3509-3514.

Article submitted: October 6, 2013; Peer review completed: November 23, 2103; Revised version received and accepted: November 30, 2013; Published: December 5, 2013.